Now you see me, now you don't: Modulation of neural responses to targets moving in three-dimensional optic flow

Sarah Nicholas[1] and Karin Nordström[1,2]*

[1]Centre for Neuroscience, Flinders University, GPO Box 2100, Adelaide, SA, 5001, Australia

[2]Department of Neuroscience, Uppsala University, Box 593, 751 24 Uppsala, Sweden

*email: karin.nordstrom@flinders.edu.au

ORCIDs

Sarah Nicholas: 0000-0002-5555-9421

Karin Nordström: 0000-0002-6020-6348

Abstract

For the human observer, it is difficult to follow the motion of small objects, especially when these are displayed against background motion. However, insects efficiently do this, as evidenced by their ability to capture prey, pursue conspecifics or defend territories, often in foliage-rich areas. This ability has been attributed to insect optic lobe neurons sharply tuned to target motion, as these respond robustly to targets even against moving backgrounds. However, their presumed post-synaptic counterparts, the target selective descending neurons (TSDNs), do not, suggesting inhibition by widefield motion. Importantly, though, previous experiments used panoramic background images, which not only lacked 3D cues, but also high-contrast features, experienced in natural flight. To mitigate this, we here use widefield motion consisting of many targets moving coherently to simulate the type of 3D optic flow that would be generated by the animal's own motion through the world. We show that TSDNs are inhibited by syn-directional optic flow, consistent with previous findings. However, and more surprisingly, we show that TSDNs are facilitated by optic flow in the opposite direction to target motion. Our results thereby emphasize that the responses of descending neurons cannot simply be inferred from their presumed pre-synaptic counterparts.

Introduction

The survival of many animals often depends on their ability to visually detect small moving objects or targets, as these could represent predators, prey or territorial intruders. Efficient target detection is a computationally challenging task which becomes even more difficult when done against visual clutter. Despite this, many insects successfully detect small moving targets and engage in highly acrobatic pursuits, often in visually complex environments. For example, male *Eristalis tenax* hoverflies establish territories in foliage rich areas within which they act as sentry, on alert for intruders or female conspecifics, and ready to engage in pursuit as soon as a target is detected[1].

Initial target detection can be facilitated by behavioral mechanisms that make the surrounding background stationary, thereby making the target stand out as the only thing that moves. For example, many insects and vertebrates alike visualize prey or conspecifics against the bright sky[2], or from a stationary stance, such as perching[3-5] or hovering[6,7]. However, as soon as the pursuer moves its own head or body, this creates self-generated optic flow[8]. To achieve reliable and continuous identification of a target, the independent motion of the target needs to be discriminated from such self-generated optic flow. That insects do this successfully is a remarkable feat considering their small brains and low-resolution compound eyes[9]. This suggests a high level of optimization, which makes insects excellent for understanding the underlying neural mechanisms.

Predatory dragonflies and territorial hoverflies, which both pursue targets, have sharply size-tuned small target motion detector (STMD) neurons in their optic lobes[10,11]. Impressively, some STMD neurons respond robustly to targets in clutter, even without

54 relative velocity differences[11,12], suggesting that they could support behavioral pursuit
55 against self-generated optic flow. However, the target selective descending neurons
56 (TSDNs), which are thought to be post-synaptic to STMDs[13], do not respond to targets
57 moving across syn-directional background motion[14]. This is peculiar as descending neurons
58 are more likely to directly drive behavioral output[15,16].

59 However, the STMDs that respond most robustly to targets against background motion, in
60 both hoverflies and dragonflies[11,12], do not project to pre-motor areas, but contralaterally
61 through the protocerebrum, with outputs in the heterolateral lobula[11,17]. This suggests a
62 role in modulating the responses of other optic lobe neurons, rather than providing direct
63 input to descending neurons[13]. In contrast, the STMDs that are more likely to provide direct
64 input to the TSDNs, based on their small receptive fields, and outputs in pre-motor areas of
65 the lateral mid- brain[18], where at least in the dragonfly, TSDNs have input dendrites[19,20], are
66 inhibited by background motion. Indeed, the response to a target moving against syn-
67 directional background motion is smaller than the response to a target traversing a white
68 background[18].

69 The TSDN response to targets against background motion is inversely correlated with the
70 response of optic flow sensitive descending neurons to the same background motion[14]. This
71 suggests that the target detection pathway is inhibited by input from the widefield system,
72 possibly post-synaptic to the STMDs. Importantly, however, the backgrounds used in
73 previous STMD[11,12,18] and TSDN[14] experiments consisted of panoramic images that were
74 displaced across the visual monitor. Most often, these were moved horizontally, with a
75 black, high-contrast target also moving horizontally. Even if the backgrounds had spatial
76 image statistics resembling nature[21] they lacked the high-contrast, hard edges of the target.

77 Where high-contrast features are present in naturalistic backgrounds, these will often
78 generate STMD responses[12]. Furthermore, the backgrounds lacked the depth cues inherent
79 in self-generated optic flow. This is crucial as self-generated optic flow not only reflects the
80 speed and direction of the animal's own movements, but also the distance to objects within
81 the environment[8]. During translational movements, for example, nearby objects move
82 faster across the retina than distant objects do. By contrast, in rotational optic flow all
83 surrounding objects move across the retina at a constant velocity, irrespective of their
84 distance from the viewer. Many insects use this information to estimate object size and
85 distance. For example, walking *Drosophila* use this to estimate relative distance prior to
86 approaching the nearest object[22], bees discern the height of objects prior to landing[23] and
87 locusts and praying mantises assess distance before attacking prey[24-26]. Hoverflies can move
88 in nearly every direction, including backwards[27,28], and in doing so generate different types
89 of translational and rotational optic flow. However, a flat, artificial image sliding across a
90 visual monitor[11,12,14,18] provides none of these relative motion cues, and none or very few
91 high-contrast cues, which would be experienced during such natural behaviors.

92 To redress this deficiency, we quantified the responses of *Eristalis* TSDNs to targets moving
93 against 6 types of optic flow, three translations and three rotations. By calibrating for the
94 hoverfly's position relative to the visual monitor, the simulated optic flow[29] mimics the self-
95 generated optic flow seen during motion through a 3D world. For this purpose, we used an
96 optic flow stimulus consisting of many targets moving coherently. The individual features
97 that make up the optic flow thus contain the same high-contrast edges as the target itself,
98 against which the target's motion can only be determined by its independent trajectory. We
99 found that this optic flow alone did not generate any TSDN response, despite it consisting of

100 similar "targets", even when moving in the neuron's preferred direction. Consistent with
101 previous results[14] we found that optic flow in the same direction as the target inhibits the
102 TSDN response. Importantly, this inhibition occurs even if the optic flow only precedes the
103 target motion and does not appear concurrently. By quantifying responses to different
104 target and background combinations, we show that the inhibition is likely inherited from
105 pre-synaptic STMDs, instead of occurring post-synaptic to the STMDs as we previously
106 suggested[14]. More surprisingly, though, we show for the first time that optic flow in the
107 opposite direction to target motion increases the TSDN response. Together, our results
108 emphasize that the responses of descending neurons cannot simply be inferred from their
109 presumed pre-synaptic counterparts in the optic lobes, and if we want to understand the
110 neural correlate of behavior we need to study the neurons closer to motor output.

111 Results

112 *TSDN responses to small targets are slightly reduced by stationary background clutter*

113 We recorded extracellularly from target selective descending neurons (TSDNs) in male
114 *Eristalis* hoverflies. TSDNs respond selectively to the motion of small targets[14,29], as shown in
115 the example where a round, black target traverses a white background (Extended Data
116 Movie 1, 2, Fig. 1a, b, blue line indicates target motion). As shown previously[14,29], TSDNs
117 typically have no spontaneous activity (Fig. 1b).

118 We used a 3D optic flow stimulus built of many targets that move coherently[29] to simulate
119 the types of retinal flow fields experienced during self-generated optic flow. Against this
120 optic flow, the target can only be identified by its independent trajectory. When the optic
121 flow and the target are both stationary, there are no spatial differences which would permit

122 the identification of the target (Fig. 1a, right). The stationary optic flow, which appeared
123 0.5 s prior to target motion, sometimes evokes 1-2 spikes (beginning of red line, Fig. 1b,
124 right, Extended Data Fig. 1, “Stationary”). Nevertheless, when the target moves across this
125 stationary optic flow (Extended Data Movie 3, 4, Fig. 1a, right), the TSDN response remains
126 robust compared with targets moving across the white background (Fig. 1b, c, compare left
127 and right data).

128 The responses of an individual TSDN are stable over long recording times, as illustrated in
129 the spike raster plot from 18 trials spanning over 22 minutes’ recording in the same neuron
130 (Fig. 1d). The resulting spike histograms highlight how similar the responses are whether the
131 target traverses a white background or the stationary optic flow (Fig. 1e). For quantification
132 across neurons, we calculated the mean spike frequency for the duration of target motion,
133 after excluding the first and last 40 ms (analysis window indicated by dotted box, Fig. 1c-e).
134 Using this, we find that there is a small response reduction to targets moving across
135 stationary optic flow (grey, Fig. 1f) compared with a white background (black, Fig. 1f).

136 We find that the response across neurons is highly variable (coefficient of variation 49% and
137 51%, respectively, Fig. 1f). This could reflect the internal state of the individual animals or
138 correspond to a real difference between TSDNs. In dragonfly TSDNs, spike rates vary not
139 only across neuron types, but also within neuron types[19,30]. To take this variability into
140 account, subsequent data from each neuron are normalized to its own mean response to a
141 target moving across a white background (black, Fig. 1f).

142

143 ***The TSDN response to target motion is strongly affected by sideslip and yaw optic flow***

144 We next investigated how TSDNs respond to targets moving across either sideslip or yaw
145 optic flow. Importantly, both sideslip and yaw result in horizontal motion in the frontal
146 visual field. The control data from one TSDN show the response to a target moving over
147 stationary optic flow (grey, Fig. 2a). For each neuron, we normalized this to its mean
148 response to a target moving over a white background (grey, Fig. 2b). When the target moves
149 over sideslip optic flow in the same direction as the target, the TSDN response is strongly
150 inhibited, as seen in the example neuron (Fig. 2a) and across neurons (Fig. 2b, "Sideslip
151 +50"). We found that yaw optic flow moving in the same direction as the target, also
152 strongly inhibits the TSDN response, as seen in the example neuron (Fig. 2a) as well as
153 across neurons (Fig. 2b, "Yaw +50"). This complete inhibition is striking considering that the
154 target moved along an independent trajectory from the remaining optic flow (Extended
155 Data Movie 5, 6), but consistent with previous work using sliding background images[14].

156 When the sideslip optic flow moves in the opposite direction to the target the TSDN
157 response is strongly enhanced (Extended Data Movie 7, 8, Fig. 2a, "Sideslip -50"). This
158 response increase to target motion against sideslip optic flow in the opposite direction is
159 substantial (mean 71.1%) and consistent across neurons (Fig. 2b). Similarly, yaw optic flow
160 in the opposite direction to the target also facilitates the TSDN response by 84.9%, as seen
161 in the example data (Fig. 2a) and across neurons (Fig. 2b, "Yaw -50"). Such response
162 facilitation was not seen when displaying targets moving over panoramic background
163 images, in either TSDNs[14] or target tuned neurons in the fly optic lobes[11,18,31].

164 The background optic flow itself, contained ca. 1200 “targets” moving coherently in front of
165 the fly. When the sideslip moves in the TSDN’s preferred direction (Fig. 2, “Sideslip +50”) we
166 expect tens of these “background targets” to move through the receptive field of the TSDN
167 (Extended Data Movie 5, 6). Despite this, across 222 repetitions in 12 TSDNs, preferred
168 direction sideslip optic flow generated a response in only 18% of the repetitions (Extended
169 Data Fig. 1a, “Sideslip +50”). In the instances where preferred direction sideslip optic flow
170 generated a response, the amplitude of the response was less than one-fifth of the response
171 to a target traversing a white background (Extended Data Fig. 1b, “Sideslip +50”). In
172 addition, when the background sideslips in the anti-preferred direction, we see small
173 breakthrough responses in 9% of repetitions (213 repetitions, “Sideslip -50”, Extended Data
174 Fig. 1). Taken together, this suggests that the coherent motion of the background is treated
175 differently from the independent motion of a target.

176 ***The response to targets moving against other types of 3D optic flow is inhibited***

177 We next investigated the effect different types of 3D optic flow has on TSDN responses to
178 target motion. The example data from one TSDN show that the response to targets is more
179 strongly inhibited by lift optic flow moving downwards in the visual field (Fig. 3a, “Lift +50”)
180 compared to lift moving upwards (Fig. 3a, “Lift -50”). Across neurons, however, both
181 directions of lift optic flow suppress the TSDN response (by 44.0%, “Lift +50”; and 34.2%,
182 “Lift -50”, Fig. 3b). When the target is instead displayed again pitch optic flow, which
183 provides similar vertical, local motion in the frontal visual field, the response is suppressed
184 by similar levels (57.1%, “Pitch +50”, and 54.9%, “Pitch -50”, Fig. 3b). In addition, the
185 response to target motion is inhibited to roughly similar levels when displayed against
186 thrust or roll optic flow in either direction (Fig. 3).

187 In summary, when displaying a target moving horizontally in the TSDN's preferred direction,
188 optic flow in the opposite direction facilitates the response, syn-directional optic flow
189 completely inhibits the response, and optic flow in any other direction inhibits the response
190 by ca. 50% (Fig. 2, 3). The relative lack of responses to the optic flow itself can be seen in
191 Extended Data Fig. 1.

192 ***TSDN responses to target motion is inhibited by preceding optic flow***

193 In dragonflies, STMD responses to target motion can be primed by preceding target motion,
194 thus facilitating responses to longer target trajectories[32,33]. Above, we showed that TSDN
195 responses to target motion are affected by sideslip optic flow (Fig. 2). To determine if this
196 effect can be primed in a similar manner, we moved preceding optic flow for 1 s (green, Fig.
197 4a), but stopped it to be stationary (red, Fig. 4a) concurrent with target motion (blue, Fig.
198 4a).

199 In the control experiment the optic flow was stationary preceding and concurrent with
200 target motion (grey, Fig. 4b). We found that when sideslip optic flow preceded target
201 motion in the same direction, this was enough to significantly inhibit the TSDN response,
202 even if the optic flow concurrent with target motion was stationary (black, Fig. 4b). This
203 suggests that the inhibition of TSDN responses can be primed by preceding optic flow. We
204 did the inverse experiment where the sideslip optic flow moves concurrently with target
205 motion and we varied the preceding optic flow. We found that whether the optic flow was
206 in motion or stationary prior to the target had no significant effect on the TSDN inhibition
207 (Fig. 4c).

208 We next investigated whether facilitation by sideslip optic flow in the opposite direction to
209 target motion can be primed. We found that preceding sideslip optic flow in the opposite
210 direction to target motion did not increase the TSDN response (black, Fig. 4d) compared to
211 control (grey, Fig. 4d). When the sideslip optic flow moves in the opposite direction
212 concurrent with target motion, the TSDN response is facilitated (Fig. 4e). However, whether
213 the sideslip was in motion or was stationary prior to the target had no significant effect on
214 this TSDN facilitation (Fig. 4e).

215 ***TSDN inhibition by syn-directional optic flow is likely inherited from pre-synaptic STMDs***

216 The data above show that TSDN responses to horizontal target motion are almost
217 completely inhibited if the optic flow moves in the same direction as the target (Fig. 2), and
218 by 34% if displayed against lift, which moves perpendicular to the target (grey crosses, Fig.
219 5c, d, re-plotted from Fig. 2b, 3b). This suggests that the target detection pathway receives
220 inhibitory input from widefield motion. We assume that TSDNs receive input from
221 STMDs[11,18] or other target tuned neurons[31,34-36], potentially directly (dashed lines,
222 pictograms, Fig. 5c, d). Inhibition from widefield motion could take place post-synaptic to
223 the STMDs, but pre-synaptic to TSDNs (pictogram, Fig. 5c). If so, we would not expect the
224 normalized TSDN responses to change if the target changes direction, but the optic flow
225 remains the same (black lines, Fig. 5d). In this scenario, the TSDN inhibition would be
226 correlated with the optic flow, irrespective of target direction. Alternatively, inhibition from
227 the widefield motion could take place prior to the pre-synaptic STMDs, so that the STMDs
228 themselves are unable to respond to targets against syn-directional background motion
229 (pictogram, Fig. 5d). This could e.g. be caused by direct inhibition from widefield motion, or
230 from the underlying model generating target selectivity itself. If this is true, the TSDN

231 response would be most strongly inhibited when target and optic flow move in the same
232 direction, whereas targets moving perpendicular to the optic flow would be more
233 detectable (black lines, Fig. 5d).

234 To investigate these two hypotheses we recorded from TSDNs that respond robustly not
235 only to horizontal target motion (grey, Fig. 5a, b), but also to vertical target motion (black,
236 Fig. 5a, b). As before, we found that when the target moves horizontally against sideslip
237 optic flow in the same direction as the target, the response is strongly inhibited (left, Fig.
238 5e). When the target instead moves vertically but the optic flow remains horizontal, so that
239 the target now moves perpendicular to the optic flow, the TSDN response is significantly
240 larger (right, Fig. 5e). In the inverse experiment, when the target moves against lift optic
241 flow, the TSDN response is more strongly inhibited when the target moves in the same
242 direction (right, Fig. 5f), compared with when the target moves horizontally (left, Fig. 5f).
243 These results therefore support our second hypothesis (Fig. 5d), that the inhibition by
244 widefield motion is inherited from the pre-synaptic STMDs, or other target tuned neurons.

245 ***TSDN response facilitation by background motion is linked to target direction***

246 Above, we showed that inhibitory input from the widefield motion system is likely inherited
247 from the pre-synaptic STMDs (Fig. 5). To determine if facilitation (Fig. 2, 3) could also be
248 caused by input from the widefield system, we tested the analogous two hypotheses in the
249 same neurons as Figure 5. If facilitation takes place post-synaptic to the STMDs (pictogram,
250 Fig. 6a), we would expect the TSDN facilitation to be correlated with the optic flow,
251 irrespective of target direction (black lines, Fig. 6a). Alternatively, if facilitation takes place
252 prior to the pre-synaptic STMDs (pictogram, Fig. 6b), the TSDN response would be stronger

253 when target and background move in the opposite direction compared to targets moving
254 perpendicular to the optic flow (black lines, Fig. 5d).

255 We found that when the target moves horizontally with the background side-slipping in the
256 opposite direction to the target, the response is significantly larger compared to the
257 response to a vertical target on the same optic flow (Fig. 6c). In the inverse experiment,
258 when we display targets against lift optic flow, there was no difference depending on the
259 direction of the target (Fig. 6d). There is thus no significant facilitation when the target
260 moves vertically against lift optic flow in the opposite direction (right, Fig. 6d). Taken
261 together, our data (Fig 6c, d) do not support either hypothesis (Fig. 6a, b) making it unclear
262 where the facilitation by optic flow comes from (Fig. 2, 3, 6).

263 Discussion

264 We generated optic flow using the coherent motion of thousands of "targets" within a
265 simulated 3D space surrounding the hoverfly, and projecting the can 1200 targets anterior
266 of the fly onto a 2D visual monitor[29]. We showed that this 3D optic flow stimulus modulates
267 the TSDN response to target motion. In particular, we found that optic flow in the opposite
268 direction to target motion strongly enhances the TSDN response, that optic flow in the same
269 direction virtually abolishes the TSDN response, and that other types of optic flow decrease
270 the TSDN response to a lesser degree (Fig. 2, 3). We found that preceding syn-directional
271 optic flow was enough to inhibit the TSDN response, even if the optic flow was stationary
272 during target motion (Fig. 4). Using different directions of target motion and optic flow, we
273 showed that the inhibition by is likely inherited from the STMDs (Fig. 5), but that the source
274 of the facilitation remains unclear (Fig. 6).

275 ***TSDN input***

276 The pre-synaptic input of TSDNs has not been verified, but is likely to come from target-
277 tuned neurons in the optic lobes[13]. Our experiments changing the direction of target motion
278 and optic flow (Fig. 5) suggests that the lack of TSDN responses to targets against syn-
279 directional optic flow is inherited from the pre-synaptic neurons. Indeed, early target
280 motion models relied on inhibitory feedback from the widefield system[37]. This is
281 conceptually an appealing model, as by simply subtracting self-generated background
282 motion, the independent motion of a target will stand out[38-40]. This model explains
283 physiological responses of blowfly lobula plate Figure Detecting (FD) cells, where the
284 response to small object motion is inhibited by background motion in the same and in the
285 opposite direction[39]. However, as FD cells are not as sharply tuned to small targets as TSDNs
286 are[37], and FD cells often respond to features within the background[41], as opposed to TSDNs
287 (Extended Data Fig. 1) they are unlikely to provide the TSDN input.

288 As some STMDs respond robustly to targets moving in visual clutter, even without relative
289 motion cues, they cannot rely on the FD model, which prompted the development of an
290 elementary STMD model[42]. The elementary STMD model uses the unique spatiotemporal
291 profile created by the motion of a dark target where its leading edge creates a dark contrast
292 change (OFF), quickly followed by the bright contrast change (ON) of the target's trailing
293 edge. By separating and half-wave rectifying the ON and OFF contrast signals from the same
294 point in space, and adding lateral inhibition from neighboring channels, a selective response
295 to small, dark, moving targets is generated[42]. The elementary STMD model provides robust
296 predictions of physiological responses of dragonfly STMDs[12,43]. However, as we see strong
297 inhibition of the TSDN target response when targets move over syn-directional optic flow

298 (Fig. 2, 3), and this inhibition takes place pre-synaptic to the TSDNs (Fig. 5), this argues
299 against TSDN input from an elementary STMD type model.

300 Importantly, as well, the elementary STMD model predicts[42] that background features with
301 the correct spatio-temporal profile will generate a neural response. Indeed, this prediction
302 is confirmed in dragonfly STMD recordings[12]. In our TSDN experiments the background
303 consisted of hundreds of targets moving coherently (Fig. 1a)[29]. Therefore, we expect tens of
304 these to move through the TSDN receptive field at any one time. These targets have varying
305 size, from the smallest we can render on our screen (1 pixel, below the resolution of the
306 hoverfly eye[44]) to 37° diameter, larger than what we expect TSDNs to respond to[14].
307 Nevertheless, when the optic flow moves in the neuron's preferred direction we would
308 expect some of these targets to have the right size to trigger a TSDN response, if the STMD
309 model underlies TSDN tuning. However, the lack of strong, and even consistent responses to
310 "targets" in preferred direction optic flow ("Sideslip +50", "Yaw +50", Extended Data Fig. 1),
311 also argue against an elementary STMD model type input to the TSDNs.

312 STMDs and FD cells are not the only object tuned neurons in the fly optic lobes. In
313 *Drosophila*, lobula columnar (LC) neurons have recently received more attention as possible
314 substrates of figure-ground discrimination behaviors[45]. Whereas some of these respond
315 better to bars than to small objects, LC11 and LC26 appear to respond selectively to small
316 targets[31,46]. Indeed, as LC11 neurons are clearly size-tuned, they would physiologically
317 classify as STMDs[47], and might be the *Drosophila* correlates of the columnar small-field
318 STMDs described in *Eristalis*[18]. LC11 neurons are especially interesting as they are clearly
319 involved in behavioral responses to small objects[36]. A model based on LC11 physiology
320 generates small object selectivity using a combination of center-surround antagonism and

321 rapid adaptation[36]. Indeed, LC11 neurons are strongly inhibited by background motion, and
322 this inhibition is believed to take place upstream of LC11[35], i.e. consistent with our
323 conceptual model (Fig. 5b). However, arguing against LC11 providing input to TSDNs is the
324 finding that they are equally inhibited by background motion in the same as well as in the
325 opposite direction to object motion[34], inconsistent with TSDNs (Fig. 2). In addition, LC11
326 neurons are not directional[35,46], so if they provide the input to the TSDNs, directionality has
327 to be added at some stage.

328 STMDs are a very heterogeneous group[11]. Some STMDs' responses to target motion are
329 slightly inhibited by syn-directional background motion[18], and other STMDs even respond
330 weakly to features in the background[11], but a complete lack of response to targets in clutter
331 are unpublished. More work on the pre-synaptic input to the TSDNs is clearly needed,
332 linking any variability in ability to see targets in clutter with neuro-anatomy, to determine
333 which neurons provide direct input to the TSDNs that we recorded from here.

334 ***Behavioral relevance***

335 The facilitation of TSDN responses to target motion displayed on optic flow in the opposite
336 direction (Fig. 2b) is a novel observation, and difficult to reconcile with the existing models
337 of small target selectivity discussed above[36,39,42]. Indeed, whereas the inhibition is clearly
338 inherited from the pre-synaptic STMDs (Fig. 5), it is unclear where the facilitation is
339 generated (Fig. 6). Interestingly, we only saw facilitation to horizontal target motion (Fig. 2,
340 6), and not to vertical target motion (Fig. 6d), even if the neurons clearly respond to these
341 targets (Fig. 5a, b). Furthermore, whereas inhibition could be primed by preceding motion

342 (Fig. 4b), facilitation could not (Fig. 5c, e). All of these experiments (Fig. 4-6) point to
343 facilitation being generated somewhere else than inhibition.

344 Our own previous work, using panoramic background images, showed that TSDN responses
345 to small targets are significantly reduced when the target and the background move in
346 opposite direction[14]. This suggests that there is something fundamentally different about
347 the image background used previously[14] and the 3D optic flow used here. Indeed, the 3D
348 optic flow used here consisted of "targets" moving coherently (Extended Data Movie 5-8),
349 so that the target itself is impossible to identify in a stationary screen shot (Fig. 1a).
350 Furthermore, 3D depth cues are important for many insects[22,23,25], but not available when
351 viewing flat images. These differences could underlie the facilitation of TSDN responses.

352 Nevertheless, the facilitation could make behavioral sense. Prior to initiating target pursuit,
353 male *Eristalis* hoverflies predict the flight course required to successfully intercept the
354 target. This prediction is predominantly based on the angular velocity of the target[48]. To
355 successfully execute an interception style flight course, the hoverfly turns in the direction
356 that the target is moving[48]. In doing so, the hoverfly creates self-generated optic flow in the
357 opposite direction to the target's motion. If the TSDNs that we have recorded from here are
358 involved in such planning of pursuit, they would be facilitated when the target moves in the
359 opposite direction to the self-generated optic flow (Fig. 2, 3), which might be beneficial.

360 Once an interception style pursuit has started, if it is perfect the target's position remains
361 fixed on the pursuer's eye. If the retinal position of the target slips, male *Syritta* hoverflies
362 correct this by turning towards the target at an angular velocity proportional to the target's
363 angular position on the eye[28]. Such turns towards the target could generate optic flow in

364 different directions depending on the target's angular position. If this generates optic flow
365 in the same direction as the target is moving, the TSDNs would be inhibited (Fig. 2), likely
366 making them less suitable during flight. However, reconstructing retinal flow fields as
367 experienced during actual pursuits[49] will help resolve how often the target and the optic
368 flow actually move in the same direction. Furthermore, replaying such reconstructed
369 pursuits to TSDNs may determine whether they would respond during actual pursuits.

370 Importantly, as opposed to the case of a pursuing hoverfly, we recorded from immobilized
371 animals, with no neuronal feedback from the flight motor circuits[50,51]. It is possible that the
372 TSDN responses that we recorded are affected by the animals being immobilized. Indeed, in
373 two descending neurons types that control landing behaviors in *Drosophila,* visual responses
374 are suppressed in non-flight states[52]. Octopamine, which has been shown to mimic flight
375 behavior, restores responses in one of these neurons, while the other may receive direct
376 feedback from flight motor circuits[52]. This prevents inappropriate landing behaviors from
377 occurring during non-flight periods. Similarly, in *Drosophila*, the responses of bar tuned
378 lobula columnar LC12 and LC15 neurons are suppressed by simultaneous background
379 motion, with the effect reversed by chlordimeform, an octopamine agonist[31]. However, the
380 inability of LC11 neurons to respond to targets against backgrounds is not restored with
381 chlordimeform[31]. While technically difficult to record from TSDNs during actual flight, it
382 should be possible to mimic flight be treating the animal with chlordimeform or
383 octopamine. Another possibility is that TSDNs are not involved in active target pursuit and
384 that another class of neurons is recruited during flight. Indeed, there are other descending
385 neurons in the insect ventral nerve chord, including those that also respond to looming
386 stimuli, that respond to small targets[19,29].

387 ## Methods

388 ### *Electrophysiology*

389 *Eristalis tenax* hoverflies were reared and maintained as previously described[53]. Prior to
390 electrophysiology, the male hoverfly was immobilized ventral side up using a beeswax and
391 resin mixture. A small hole was cut at the anterior end of the thorax to expose the cervical
392 connective, which was then raised slightly and supported using a small wire hook. A sharp
393 polyimide-insulated tungsten microelectrode (2 MOhm, Microprobes, Gaithersburg, USA)
394 was inserted into the cervical connective. The animal was grounded via a silver wire inserted
395 into the ventral part of the hole. This also served as a recording reference.

396 Extracellular signals were amplified at 100x gain and filtered through a 10- to 3000-Hz
397 bandwidth filter on a DAM50 differential amplifier (World Precision Instruments, Sarasota,
398 USA), with 50 Hz noise removed with a HumBug (Quest Scientific, North Vancouver,
399 Canada). The data were digitized via Powerlab 4/30 (ADInstruments, Sydney, Australia) and
400 acquired at 40 kHz with LabChart 7 Pro software (ADInstruments). Single units were
401 discriminated by amplitude and half-width using Spike Histogram software (ADInstruments).

402 ### *Visual stimuli*

403 *Eristalis* males were placed ventral side up, centered and perpendicular to an Asus LCD
404 screen (Asus, Taipai, Taiwan) at a distance of 6.5 cm. The screen had a refresh rate of
405 165 Hz, a linearized contrast with a mean illuminance of 200 Lux and a spatial resolution of
406 2560 x 1440 pixels, giving a projected screen size of 155° x 138°. Visual stimuli were

407 displayed using custom written software based on the Psychophysics toolbox[54,55] in Matlab
408 (Mathworks, Natick, USA).

409 TSDNs were identified as described previously[14,29]. In short, TSDNs have small receptive
410 fields located in the dorso-frontal visual field, and sharp size tuning with a peak response to
411 targets subtending 3°- 6°, with no response to larger bars, to looming or to widefield
412 stimuli[29].

413 All targets were black and round with a diameter of 15 pixels, moving at a velocity of
414 900 pixels/s for 0.48 s. When converted to angular values and taking the small frontal
415 receptive fields of TSDNs into account, this corresponds to a diameter of 3° and a velocity of
416 130°/s[14]. Unless otherwise stated, each target trajectory travelled in each neuron's
417 preferred direction and across the center of its receptive field. Between repetitions, we
418 varied the target elevation slightly, to minimize habituation[14]. A minimum of 4 s was left
419 between stimulus presentations. Stimulus order was randomized.

420 3D optic flow was generated as previously described[29]. Briefly, the optic flow consisted of a
421 simulated 3D space, a cube with 4 m sides, filled with 2 cm diameter spheres at a density of
422 100 per m^3, with the hoverfly placed in the center. The coherent motion of these ca 6400
423 spheres around the hoverfly was used to simulate self-generated optic flow. The ca 1200
424 spheres anterior to the hoverfly were projected onto the screen, with the size of the
425 resultant circles indicating the distance from the hoverfly. Circles closer than 6 cm were not
426 displayed. Six types of optic flow were simulated: three translations at 50 cm/s (sideslip, lift
427 and thrust) and three rotations at 50°/s (yaw, pitch and roll). Unless otherwise stated optic

428 flow was displayed for 0.48 s prior to the target. Both target motion and optic flow ended
429 simultaneously.

430 ***Data analysis and statistics***

431 We recorded from 24 TSDNs in 24 male hoverflies. We kept data from all TSDNs that
432 showed a robust response to a target moving over a white background (Extended Data
433 Movie 1, 2). We repeated this control throughout the recording, and only kept data from
434 neurons that showed a consistent response to this control. We only kept data from
435 experiments with a minimum 9 repetitions. The data from repetitions within a neuron were
436 averaged, and shown as spike histograms (mean ± sem) with 1 ms resolution, after
437 smoothing with a 20 ms square-wave filter. For quantification across neurons, we calculated
438 the mean spike rate for each neuron from the spike histogram for the duration of target
439 motion, after excluding the first and last 40 ms (dotted boxes, Fig. 1b-e). Due to the
440 response variation across animals (Fig. 1f), the mean spike rate for each TSDN was
441 normalized to its own mean response to a target moving over a white background.

442 Data analysis was performed in Matlab and statistical analysis in Prism 7.0c for Mac OS X
443 (GraphPad Software, San Diego, USA). Throughout the paper *n* refers to the number of
444 repetitions within one neurons, and *N* to the number of neurons. The sample size, type of
445 test and P value is indicated in each figure legend. We performed either two-sided t-tests,
446 one-way RM ANOVAs, followed by Dunnett's post hoc test for multiple comparisons or two-
447 way RM ANOVAs, followed by either Bonferroni's or Tukey's post hoc test for multiple
448 comparisons. All data have been deposited to DataDryad.

449

Acknowledgements

We thank the Botanic Gardens of Adelaide for their ongoing support. This research was funded by the US Air Force Office of Scientific Research (AFOSR, FA9550-19-1-0294), the Australian Research Council (ARC, DP170100008, DP180100144 and FT180100289), and the Flinders Foundation.

Author Contributions

K.N. conceptualized the study and developed the research plan. Both authors designed the study. S.N. performed all experiments and data analyses and prepared the figures. Both authors wrote the manuscript and contributed to the discussion. K.N. supervised all the work.

Competing Interests Statement

The authors declare no competing interests.

References

1 Wellington, W. & Fitzpatrick, S. Territoriality in the drone fly, *Eristalis tenax* (Diptera, Syrphidae). *Can Entomol* **113**, 695-704 (1981).

2 Zeil, J. Sexual dimorphism in the visual system of flies: The free flight behavior of male Bibionidae (Diptera). *J Comp Physiol A* **150**, 395-412 (1983).

3 Fabian, S. T., Sumner, M. E., Wardill, T. J., Rossoni, S. & Gonzalez-Bellido, P. T. Interception by two predatory fly species is explained by a proportional navigation feedback controller. *Journal of The Royal Society Interface* **15** (2018).

4 Schröder, R., Linkem, C. N., Rivera, J. A. & Butler, M. A. Should I stay or should I go? Perching damselfly use simple colour and size cues to trigger flight. *Animal Behaviour* **145**, 29-37, doi:https://doi.org/10.1016/j.anbehav.2018.08.015 (2018).

5 O'Rourke, C. T., Pitlik, T., Hoover, M. & Fernández-Juricic, E. Hawk eyes II: diurnal raptors differ in head movement strategies when scanning from perches. *PLoS One* **5**, e12169, doi:10.1371/journal.pone.0012169 (2010).

6 Fitzpatrick, S. M. & Wellington, W. G. Contrasts in the territorial behavior of three species of hover flies (Diptera: Syrphidae). *Can Entomol* **115**, 559-566 (1983).

7 Corvidae, E. L., Bierregaard, R. O. & Peters, S. E. Comparison of wing morphology in three birds of prey: correlations with differences in flight behavior. *J Morphol* **267**, 612-622, doi:10.1002/jmor.10425 (2006).

8 Koenderink, J. J. Optic flow. *Vision Res* **26**, 161-179, doi:10.1016/0042-6989(86)90078-7 (1986).

9 Land, M. F. Visual acuity in insects. *Annu Rev Entomol* **42**, 147-177, doi:DOI 10.1146/annurev.ento.42.1.147 (1997).

485 10 O'Carroll, D. Feature-detecting neurons in dragonflies. *Nature* **362**, 541-543 (1993).
486 11 Nordström, K., Barnett, P. D. & O'Carroll, D. C. Insect detection of small targets
487 moving in visual clutter. *PLoS Biol* **4**, 378-386 (2006).
488 12 Wiederman, S. D. & O'Carroll, D. C. Discrimination of features in natural scenes by a
489 dragonfly neuron. *J Neurosci* **31**, 7141-7144, doi:10.1523/JNEUROSCI.0970-11.2011
490 (2011).
491 13 Nordström, K. Neural specializations for small target detection in insects. *Curr Opin*
492 *Neurobiol* **22**, 272-278, doi:S0959-4388(11)00231-5 [pii]
493 10.1016/j.conb.2011.12.013 [doi] (2012).
494 14 Nicholas, S., Supple, J., Leibbrandt, R., Gonzalez-Bellido, P. T. & Nordström, K.
495 Integration of small- and wide-field visual features in Target-Selective Descending
496 Neurons of both predatory and non-predatory dipterans. *J Neurosci* **38**, 10725-
497 10733, doi:10.1523/jneurosci.1695-18.2018 (2018).
498 15 Namiki, S., Dickinson, M. H., Wong, A. M., Korff, W. & Card, G. M. The functional
499 organization of descending sensory-motor pathways in *Drosophila*. *eLife* **7**, e34272,
500 doi:10.7554/eLife.34272 (2018).
501 16 Chen, C. L. *et al.* Imaging neural activity in the ventral nerve cord of behaving adult
502 *Drosophila*. *Nat Commun* **9**, 4390, doi:10.1038/s41467-018-06857-z (2018).
503 17 Geurten, B. R. H., Nordström, K., Sprayberry, J. D. H., Bolzon, D. M. & O'Carroll, D. C.
504 Neural mechanisms underlying target detection in a dragonfly centrifugal neuron. *J*
505 *Exp Biol* **210**, 3277-3284, doi:doi: 10.1242/jeb.008425 (2007).
506 18 Barnett, P. D., Nordström, K. & O'Carroll, D. C. Retinotopic organization of small-
507 field-target-detecting neurons in the insect visual system. *Curr Biol* **17**, 569-578
508 (2007).

19 Gonzalez-Bellido, P. T., Peng, H., Yang, J., Georgopoulos, A. P. & Olberg, R. M. Eight pairs of descending neurons in the dragonfly give wing motor centers accurate population vector of prey direction. *Proc Natl Acad Sci USA* **110**, 676-701, doi:www.pnas.org/cgi/doi/10.1073/pnas.1210489109 (2013).

20 Olberg, R. M. Object- and self-movement detectors in the ventral nerve cord of the dragonfly. *J Comp Physiol A* **141**, 327-334 (1981).

21 Dyakova, O., Lee, Y.-J., Longden, K. D., Kiselev, V. G. & Nordström, K. A higher order visual neuron tuned to the spatial amplitude spectra of natural scenes. *Nat Commun* **6**, 8522, doi:10.1038/ncomms9522 (2015).

22 Schuster, S., Strauss, R. & Gotz, K. G. Virtual-reality techniques resolve the visual cues used by fruit flies to evaluate object distances. *Curr Biol* **12**, 1591-1594, doi:10.1016/s0960-9822(02)01141-7 (2002).

23 Lehrer, M., Srinivasan, M. V., Zhang, S. W. & Horridge, G. A. Motion cues provide the bee's visual world with a third dimension. *Nature* **332**, 356-357, doi:10.1038/332356a0 (1988).

24 Collett, T. S. Peering - Locust Behavior Pattern for Obtaining Motion Parallax Information. *Journal of Experimental Biology* **76**, 237-241 (1978).

25 Sobel, E. C. The locust's use of motion parallax to measure distance. *Journal of comparative physiology. A, Sensory, neural, and behavioral physiology* **167**, 579-588, doi:10.1007/bf00192653 (1990).

26 Nityananda, V. *et al.* A Novel Form of Stereo Vision in the Praying Mantis. *Curr Biol* **28**, 588-593.e584, doi:10.1016/j.cub.2018.01.012 (2018).

27 Geurten, B. R., Kern, R., Braun, E. & Egelhaaf, M. A syntax of hoverfly flight prototypes. *J Exp Biol* **213**, 2461-2475, doi:213/14/2461 [pii]

533 10.1242/jeb.036079 [doi] (2010).

534 28 Collett, T. S. & Land, M. F. Visual control of flight behaviour in the hoverfly, *Syritta*
535 *pipiens* L. *J Comp Physiol A* **99**, 1-66 (1975).

536 29 Nicholas, S., Leibbrandt, R. & Nordström, K. Visual motion sensitivity in descending
537 neurons in the hoverfly. *J Comp Physiol A* **206**, 149-163, doi:10.1007/s00359-020-
538 01402-0 (2020).

539 30 Supple, J. A. *et al.* Binocular Encoding in the Damselfly Pre-motor Target Tracking
540 System. *Curr Biol* **30**, 645-656.e644, doi:10.1016/j.cub.2019.12.031 (2020).

541 31 Städele, C., Keleş, M. F., Mongeau, J. M. & Frye, M. A. Non-canonical receptive field
542 properties and neuromodulation of Feature-Detecting neurons in flies. *Curr Biol*,
543 doi:10.1016/j.cub.2020.04.069 (2020).

544 32 Wiederman, S. D., Fabian, J. M., Dunbier, J. R. & O'Carroll, D. C. A predictive focus of
545 gain modulation encodes target trajectories in insect vision. *eLife* **6**,
546 doi:10.7554/eLife.26478 (2017).

547 33 Nordström, K., Bolzon, D. M. & O'Carroll, D. C. Spatial facilitation by a high-
548 performance dragonfly target-detecting neuron. *Biol Lett* **7**, 588-592,
549 doi:rsbl.2010.1152 [pii]
550 10.1098/rsbl.2010.1152 [doi] (2011).

551 34 Keleş, M. F., Hardcastle, B. J., Städele, C., Xiao, Q. & Frye, M. A. Inhibitory
552 interactions and columnar inputs to an object motion detector in *Drosophila*. *Cell*
553 *Rep* **30**, 2115-2124.e2115, doi:10.1016/j.celrep.2020.01.061 (2020).

554 35 Keleş, M. F. & Frye, M. A. Object-detecting neurons in *Drosophila*. *Curr Biol* **27**, 680-
555 687, doi:10.1016/j.cub.2017.01.012 (2017).

36 Tanaka, R. & Clark, D. A. Object-displacement-sensitive visual neurons drive freezing in *Drosophila*. *Curr Biol*, doi:10.1016/j.cub.2020.04.068 (2020).

37 Egelhaaf, M. On the neuronal basis of figure-ground discrimination by relative motion in the visual system of the fly. III. Possible input circuitries and behavioral significance of the FD-cells. *Biol Cybern* **52**, 267-280 (1985).

38 Warzecha, A. K., Egelhaaf, M. & Borst, A. Neural circuit tuning fly visual interneurons to motion of small objects. I. Dissection of the circuit by pharmacological and photoinactivation techniques. *J Neurophysiol* **69**, 329-339, doi:10.1152/jn.1993.69.2.329 (1993).

39 Egelhaaf, M. On the neuronal basis of figure-ground discrimination by relative motion in the visual system of the fly. II. Figure-detection cells, a new class of visual interneurones. *Biol Cybern* **52**, 195-209 (1985).

40 Reichardt, W. & Poggio, T. Figure-ground discrimination by relative movement in the visual-system of the fly. Part I: Experimental results. *Biol Cybern* **35**, 81-100 (1979).

41 Liang, P., Heitwerth, J., Kern, R., Kurtz, R. & Egelhaaf, M. Object representation and distance encoding in three-dimensional environments by a neural circuit in the visual system of the blowfly. *J Neurophysiol* **107**, 3446-3457, doi:jn.00530.2011 [pii] 10.1152/jn.00530.2011 [doi] (2012).

42 Wiederman, S. D., Shoemaker, P. A. & O'Carroll, D. C. A model for the detection of moving targets in visual clutter inspired by insect physiology. *PLoS ONE* **3**, e2784, doi:10.1371/journal.pone.0002784 (2008).

43 Wiederman, S. D., Shoemaker, P. A. & O'Carroll, D. C. Correlation between OFF and ON Channels Underlies Dark Target Selectivity in an Insect Visual System. *J Neurosci* **33**, 13225-13232, doi:33/32/13225 [pii]

580 10.1523/JNEUROSCI.1277-13.2013 [doi] (2013).

581 44 Straw, A. D., Warrant, E. J. & O'Carroll, D. C. A 'bright zone' in male hoverfly (*Eristalis*
582 *tenax*) eyes and associated faster motion detection and increased contrast
583 sensitivity. *J Exp Biol* **209**, 4339-4354, doi:10.1242/jeb.02517 (2006).

584 45 Aptekar, J. W., Keles, M. F., Lu, P. M., Zolotova, N. M. & Frye, M. A. Neurons forming
585 optic glomeruli compute figure-ground discriminations in *Drosophila*. *J Neurosci* **35**,
586 7587-7599, doi:10.1523/jneurosci.0652-15.2015 (2015).

587 46 Wu, M. *et al.* Visual projection neurons in the *Drosophila* lobula link feature
588 detection to distinct behavioral programs. *eLife* **5**, e21022, doi:10.7554/eLife.21022
589 (2016).

590 47 Nordström, K. & O'Carroll, D. C. Feature detection and the hypercomplex property in
591 insects. *Trends Neurosci* **32**, 383-391, doi:S0166-2236(09)00091-5 [pii]
592 10.1016/j.tins.2009.03.004 [doi] (2009).

593 48 Collett, T. S. & Land, M. F. How hoverflies compute interception courses. *J Comp*
594 *Physiol A* **125**, 191-204 (1978).

595 49 Wardill, T. *et al.* A novel interception strategy in a miniature robber fly with extreme
596 visual acuity. *Curr Biol* **27**, 854-859 (2017).

597 50 Fujiwara, T., Cruz, T. L., Bohnslav, J. P. & Chiappe, M. E. A faithful internal
598 representation of walking movements in the Drosophila visual system. *Nat Neurosci*
599 **20**, 72-81, doi:10.1038/nn.4435 (2017).

600 51 Kim, A. J., Fitzgerald, J. K. & Maimon, G. Cellular evidence for efference copy in
601 *Drosophila* visuomotor processing. *Nat Neurosci* **18**, 1247-1255,
602 doi:10.1038/nn.4083 (2015).

603 52 Ache, J. M., Namiki, S., Lee, A., Branson, K. & Card, G. M. State-dependent
604 decoupling of sensory and motor circuits underlies behavioral flexibility in
605 *Drosophila*. *Nat Neurosci* **22**, 1132-1139, doi:10.1038/s41593-019-0413-4 (2019).
606 53 Nicholas, S., Thyselius, M., Holden, M. & Nordström, K. Rearing and long-term
607 maintenance of *Eristalis tenax* hoverflies for research studies. *JoVE*, e57711,
608 doi:doi:10.3791/57711 (2018).
609 54 Brainard, D. H. The Psychophysics toolbox. *Spatial Vision* **10**, 433-436 (1997).
610 55 Pelli, D. G. The VideoToolbox software for visual psychophysics: Transforming
611 numbers into movies. *Spatial Vision* **10**, 437-442 (1997).
612

613

614 ## Figure Legends

615 ***Figure 1. The TSDN response to target motion is robust against stationary optic flow***

616 **a,** Pictograms of the round, black target, with a diameter of 3°, traversing a white
617 background (left) or stationary optic flow (right) at 130°/s. **b,** Raw data trace from an
618 extracellular TSDN recording. Timing of stimulus presentation indicated by colored bars
619 (blue, target, and red, optic flow). **c,** Magnification of the raw data traces shown in panel **b.**
620 **d,** Spike raster of the same neuron in response to 18 repeated trials of a target on a white
621 background (left) or on stationary optic flow (right). **e,** Response shown as spike histograms
622 of the mean ± sem shown with 1 ms resolution, after smoothing with a 20 ms square-wave
623 filter. **f,** The mean spiking response of different TSDNs was significantly reduced when the
624 target moved across stationary optic flow compared with a white background (N = 24;
625 P = 0.0019, two-sided paired t-test). In **b-e** the dotted box shows the analysis window used
626 for quantification. **P < 0.01.

627 ***Figure 2. The TSDN response to target motion is affected by horizontal optic flow***

628 **a**, The response of a single TSDN to a target traversing stationary optic flow (left, grey) or
629 sideslip or yaw in either the same direction or opposite direction to the target (see red
630 pictograms). All histograms from a single TSDN (mean ± sem, n = 18) shown with 1 ms
631 resolution after smoothing with a 20 ms square-wave filter. **b**, The mean response across
632 TSDNs (N = 12) to a target traversing stationary optic flow (left, grey), or sideslip or yaw in
633 either the same direction ("+50") or opposite direction ("-50") to the target after
634 normalizing the data to the response to a target traversing a white background (one-way
635 RM ANOVA followed by Post hoc Dunnett's test: sideslip +50, P < 0.0001; sideslip -50,

636 P < 0.0001, yaw +50, P < 0.0001; yaw -50, P < 0.0001). Sideslip optic flow was shown at
637 50 cm/s and yaw optic flow at 50°/s. The line shows the mean and the filled data points are
638 from the neuron shown in panel **a**. ****P < 0.0001.

639 ***Figure 3. The TSDN response to target motion is affected by 3D optic flow***

640 **a**, The response of a single TSDN to a target traversing stationary optic flow (left, grey,
641 replotted from Fig. 2a), or different types of optic flow (see red pictograms). Translations
642 were shown at 50 cm/s and rotations at 50°/s. All histograms shown as mean ± sem (n = 18)
643 at 1 ms resolution, after smoothing with a 20 ms square-wave filter. **b**, The mean response
644 across TSDNs (N = 12) to a target traversing stationary optic flow (left, grey, replotted from
645 Fig. 2b), or different types of optic flow (one-way RM ANOVA followed by Post hoc
646 Dunnett's test: lift +50, P < 0.0001; lift -50, P = 0.0006; pitch +50, P < 0.0001; pitch -50,
647 P < 0.0001; thrust +50, P < 0.0001; thrust -50, P < 0.0001; roll +50, P = 0.0020; roll -50,
648 P < 0.0001). The lines show the mean and the filled data points are from the neuron shown
649 in panel **a**. **P < 0.01, ***P < 0.001 and ****P < 0.0001.

650 ***Figure 4. The TSDN inhibition by syn-directional sideslip can be primed***

651 **a**, Typical raw data trace from a single TSDN to a target presented on sideslip optic flow,
652 which moved in the same direction as the target prior to target presentation, then remained
653 stationary during target motion. Timing is color coded: green, preceding optic flow; red,
654 concurrent optic flow; blue, target motion. **b**, TSDN target responses are significantly
655 inhibited by preceding sideslip in the same direction as the target, compared with preceding
656 stationary optic flow (N = 7, two-way RM ANOVA followed by Post hoc Bonferroni's test:
657 P = 0.0005). **c**, There was no significant difference between TSDN responses to targets

658 moving across sideslip optic flow in the same direction, whether this moved or not
659 preceding target motion (N = 7, two-way RM ANOVA: Post hoc Bonferroni's test:
660 P = 0.4704). **d**, There was no significant difference between TSDN responses to targets
661 moving across stationary optic flow, whether this moved or not preceding target motion
662 (N = 7, two-way RM ANOVA: Post hoc Bonferroni's test: P > 0.9999). The grey data is the
663 same as in panel **b**. **e**, There was no significant difference between TSDN responses to
664 targets displayed on sideslip optic flow in the opposite direction to target motion, whether
665 the optic flow moved or not preceding target motion (N = 7, two-way RM ANOVA: Post hoc
666 Bonferroni's test: P > 0.9999). **b-e**, The lines show the mean. NS P > 0.05 and ***P < 0.001.

667 ***Figure 5. The inhibition of TSDN target responses by syn-directional sideslip comes from***
668 ***the pre-synaptic input***

669 **a**, The response of a single TSDN to a target traversing the white background horizontally
670 (left, grey) or vertically (right, black). All histograms shown as mean ± sem (n = 18) at 1 ms
671 resolution, after smoothing with a 20 ms square-wave filter. **b**, The mean spiking response
672 of the same 8 TSDNs to targets moving horizontally (grey, left) or vertically (black, right)
673 over a white background (N = 8). **c**, TSDNs are likely to receive input from STMDs (dashed
674 arrow). If the inhibition from widefield motion is post-synaptic to the STMDs, the inhibition
675 will depend on the direction of optic flow. For example, since the TSDN response is strongly
676 inhibited by sideslip optic flow (grey data, replotted from Fig. 2), changing the direction of
677 target motion should not affect this inhibition. Similarly, since the TSDN response is less
678 inhibited by lift optic flow (grey data, replotted from Fig. 3), changing the direction of target
679 motion should not affect this. **d**, If the inhibition from widefield motion is pre-synaptic to
680 the STMDs, the inhibition will depend on the direction of target motion. For example,

681 changing the target direction from horizontal (grey data, replotted from Fig. 2), to vertical
682 when displayed against sideslip optic flow, should increase the response. Similarly, changing
683 the target direction to syn-directional when displayed against lift optic flow, should increase
684 the inhibition, and decrease the response. **e**, TSDN responses to targets moving across
685 sideslip optic flow are significantly increased when the target direction changes from syn-
686 directional to vertical (N = 8, two-way RM ANOVA followed by Post hoc Tukey's test:
687 P = 0.0413). **f**, TSDN responses to targets moving across lift optic flow are significantly
688 decreased when the target direction changes from perpendicular to syn-directional (N = 8,
689 two-way RM ANOVA: Post hoc Tukey's test: P = 0.0014). **e-f**, The lines show the mean.
690 *P < 0.05 and **P < 0.01.

691 ***Figure 6. There is no facilitation to targets moving across lift optic flow***

692 **a**, If the facilitation of TSDNs is due to input from the widefield system post-synaptic to the
693 STMDs, the facilitation will depend on the direction of optic flow. For example, since the
694 TSDN response is strongly facilitated by sideslip optic flow (grey data, replotted from Fig. 2),
695 changing the direction of target motion should not affect this facilitation. Similarly, since the
696 TSDN response is not facilitated by lift optic flow (grey data, replotted from Fig. 3), changing
697 the direction of target motion should not result in any facilitation. **b**, If the facilitation is
698 inherited from the STMDs, the facilitation will depend on the direction of target motion. For
699 example, changing the target direction from horizontal (grey data, replotted from Fig. 2), to
700 vertical when displayed against sideslip optic flow, should increase the response. Similarly,
701 changing the target direction to vertical when displayed against the opposing direction of
702 lift optic flow, should increase the response. **c**, TSDN responses to targets moving across
703 sideslip optic flow are significantly decreased when the target direction changes from

moving in the opposite direction to perpendicular to the optic flow (N = 8, two-way RM ANOVA: Post hoc Tukey's test: P = 0.0017). **d**, TSDN responses to targets moving across lift optic flow are not significantly affected when the target direction changes from perpendicular to moving in the opposite direction to the optic flow (N = 8, two-way RM ANOVA: Post hoc Tukey's test: P = 0.5394) **c-d**, The lines show the mean. NS P > 0.05 and **P < 0.01

712 ## Extended Data

713 ***Extended Data Figure 1. TSDN response to 3D optic flow***

714 **a**, To determine the TSDN response to the optic flow we first quantified each neuron's
715 spontaneous rate, i.e. the response to a white background. We used this as a threshold. For
716 each neuron we then quantified the number of trials in which the response to the optic flow
717 was above this spontaneous rate. This was converted to a percentage of responses. The
718 data here show this percentage of responses across 12 TSDNs as mean ± sem. **b**, In each
719 neuron, we quantified the mean response for those trials that were classified as responders
720 (in panel **a**). This mean response was normalized to each neuron's mean response to a
721 target traversing a white background. Data are shown as mean ± sem (N = 12).

722 ***Extended Data Movie 1. TSDN response to a target over a white background***

723 The movie depicts the stimulus as displayed on the screen, with the hoverfly positioned
724 centered and perpendicular to the screen. The hoverfly was ventral side up, but we have
725 rotated the movie for display purposes for the dorsal side to be up. The colored lines show
726 the outline of the receptive field, mapped as described previously[29]. The red data at the
727 bottom of the movie show the response of an example TSDN.

728 ***Extended Data Movie 2. TSDN response to a target over a white background***

729 Same as Movie 1, but slowed down 10 times.

730

Extended Data Movie 3. TSDN response to a target over stationary optic flow

The movie depicts the stimulus as displayed on the screen, with the colored lines showing the outline of the receptive field. The red data at the bottom of the movie show the response of an example TSDN. In this case the optic flow was stationary, and appeared 0.5 s before the target.

Extended Data Movie 4. TSDN response to a target over stationary optic flow

Same as Movie 3, but slowed down 10 times.

Extended Data Movie 5. TSDN response to a target over syn-directional sideslip optic flow

The movie depicts the response of the same example TSDN to the same target motion as in previous movies, but now traversing sideslip optic flow appearing 0.5 s before the target. The hoverfly was positioned at a distance of 6.5 cm. At this viewing distance, the resulting optic flow simulates the type of optic flow that would be generated by the hoverfly sideslipping through the world at 50 cm/s. The simulated optic flow consisted of ca 6400 spheres, of which ca 1200 are projected onto the screen at any one time.

Extended Data Movie 6. TSDN response to a target over syn-directional sideslip optic flow

Same as Movie 5, but slowed down 10 times. Note the many optic flow “targets” of the correct size that move through the receptive field (colored contour lines).

Extended Data Movie 7. TSDN response to a target over opposite direction sideslip optic flow

The movie depicts the response of the same example TSDN to the same target motion as in previous movies, but now traversing sideslip optic flow in the opposite direction to the target.

Extended Data Movie 8. TSDN response to a target over opposite direction sideslip optic flow

Same as Movie 7, but slowed down 10 times.

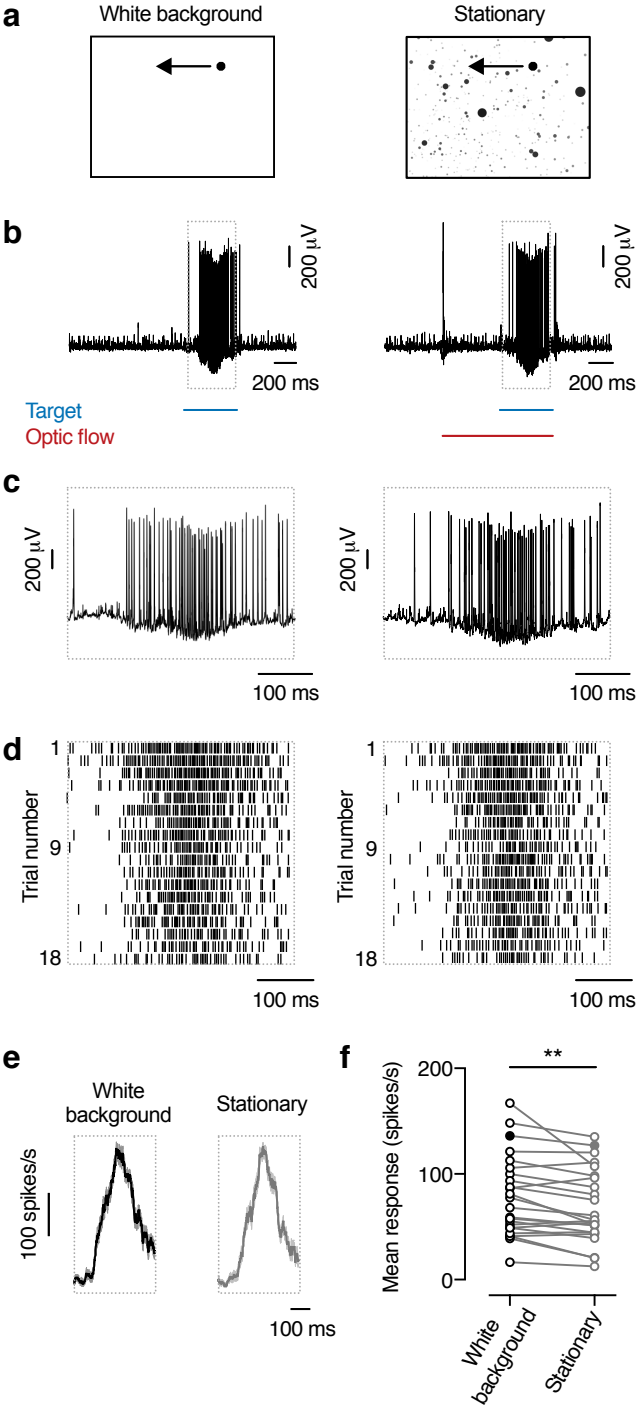
a
White background
Stationary
b
200 μV
200 ms
200 μV
200 ms
Target
Optic flow
c
200 μV
100 ms
200 μV
100 ms
d
Trial number
1
9
18
100 ms
Trial number
1
9
18
100 ms
e
White background
Stationary
100 spikes/s
100 ms
f
Mean response (spikes/s)
200
100
0
**
White background
Stationary

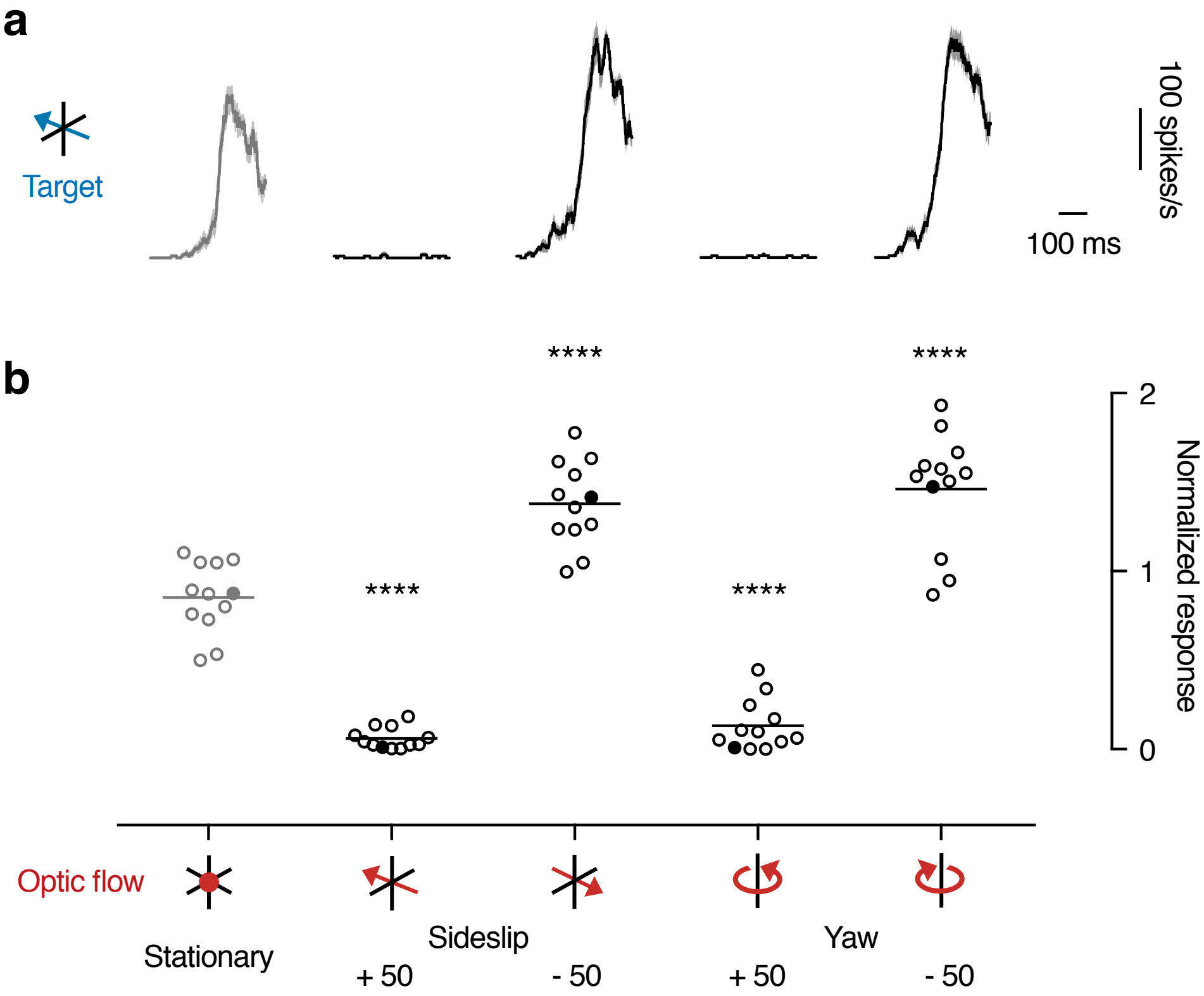
a
Target
100 spikes/s
100 ms
b
****
****
****
****
2
1
0
Normalized response
Optic flow
Stationary
Sideslip
+ 50
- 50
Yaw
+ 50
- 50

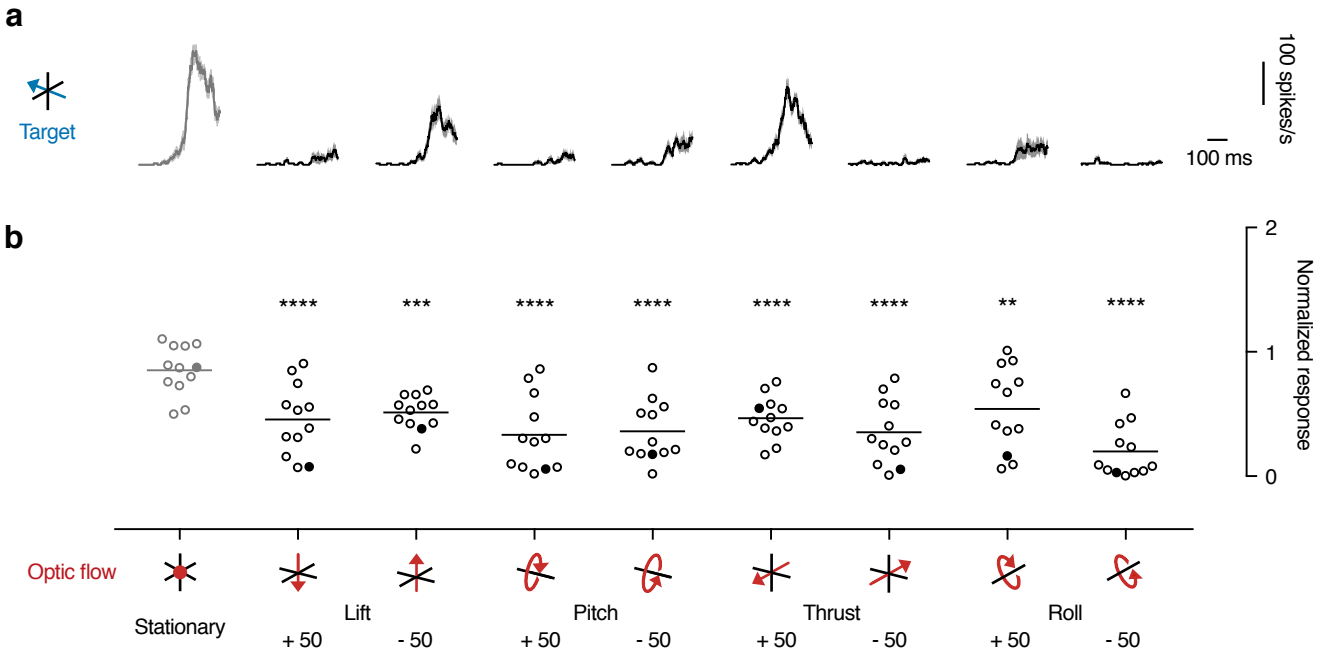
a
Target
100 spikes/s
100 ms
b
Normalized response
2
1
0
****
***
****
****
****
****
**
****
Optic flow
Stationary
Lift
+ 50
- 50
Pitch
+ 50
- 50
Thrust
+ 50
- 50
Roll
+ 50
- 50

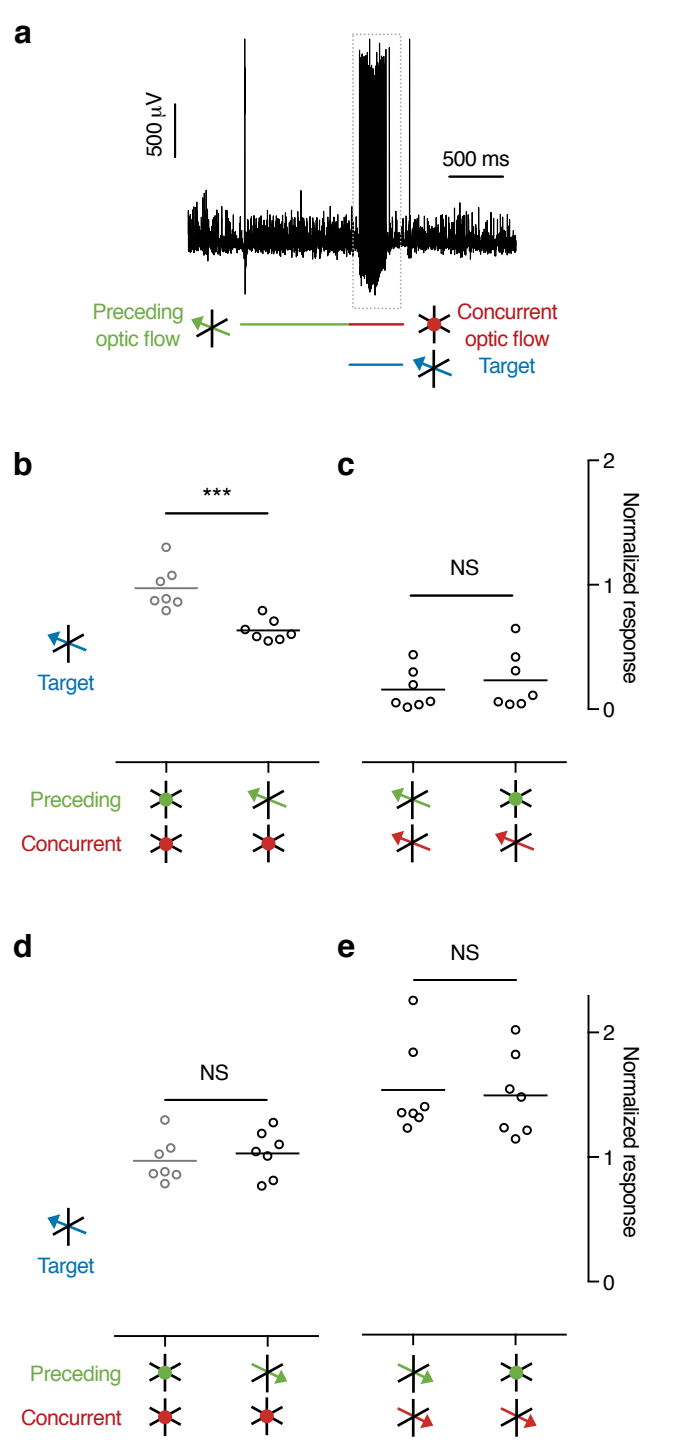
a
500 μV
500 ms
Preceding optic flow
Concurrent optic flow
Target
b
***
Target
Preceding
Concurrent
c
NS
Normalized response
2
1
0
d
NS
Target
Preceding
Concurrent
e
NS
Normalized response
2
1
0

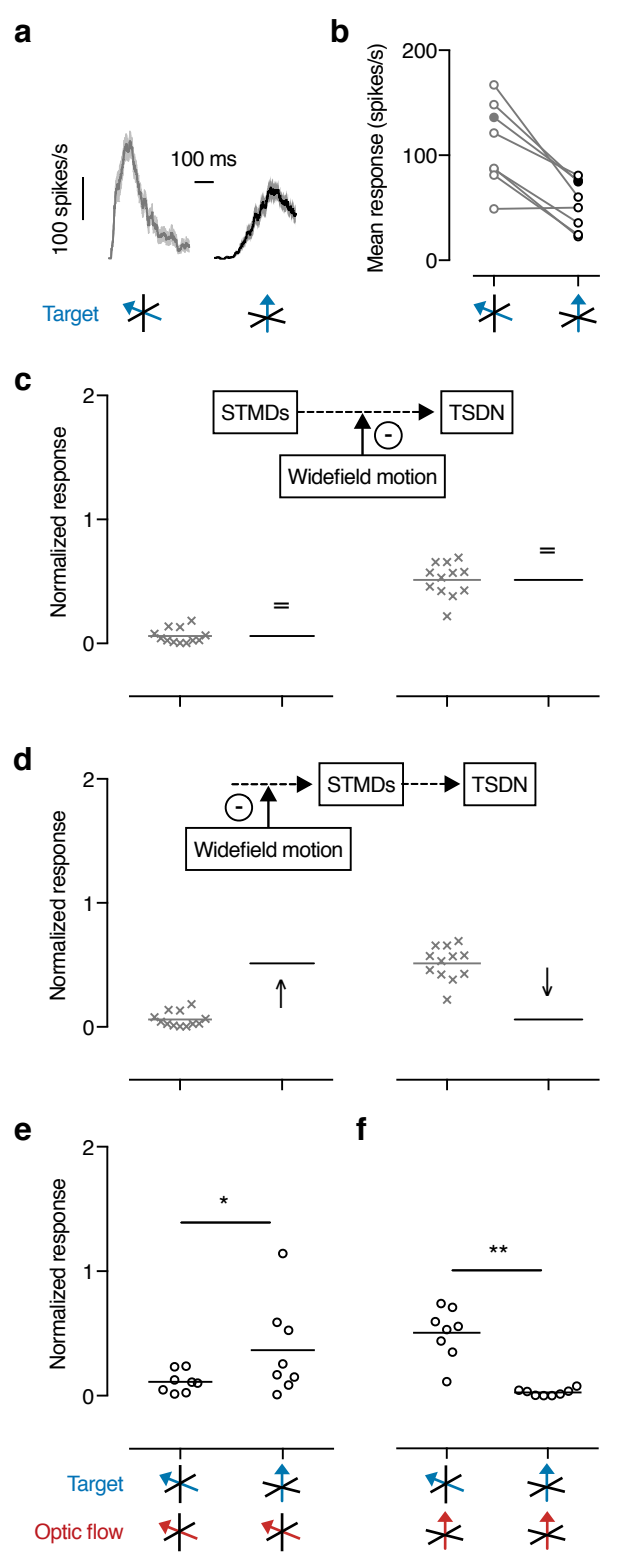
a
100 spikes/s
100 ms
Target
b
Mean response (spikes/s)
200
100
0
c
Normalized response
2
1
0
STMDs
TSDN
Widefield motion
-
=
=
d
Normalized response
2
1
0
STMDs
TSDN
Widefield motion
-
e
Normalized response
2
1
0
*
f
**
Target
Optic flow

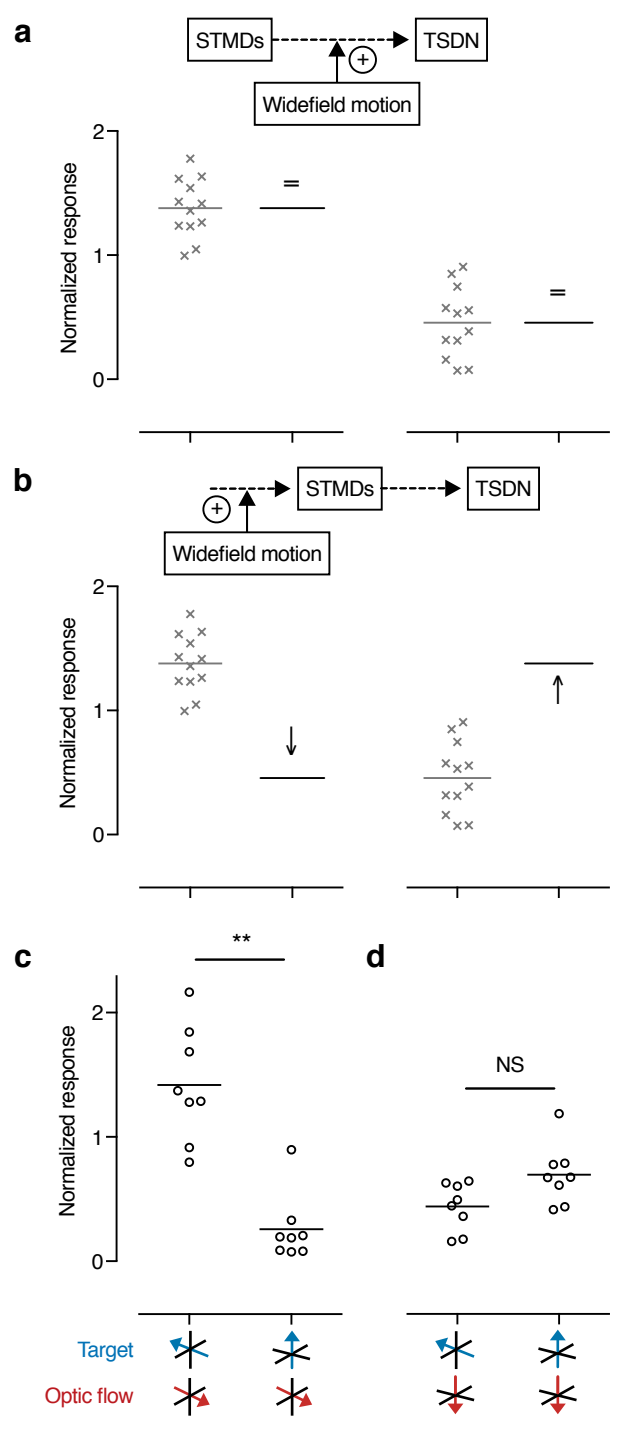
a
STMDs
TSDN
+
Widefield motion
Normalized response
2
1
0
=
=
b
STMDs
TSDN
+
Widefield motion
Normalized response
2
1
0
c
**
Normalized response
2
1
0
d
NS
Target
Optic flow

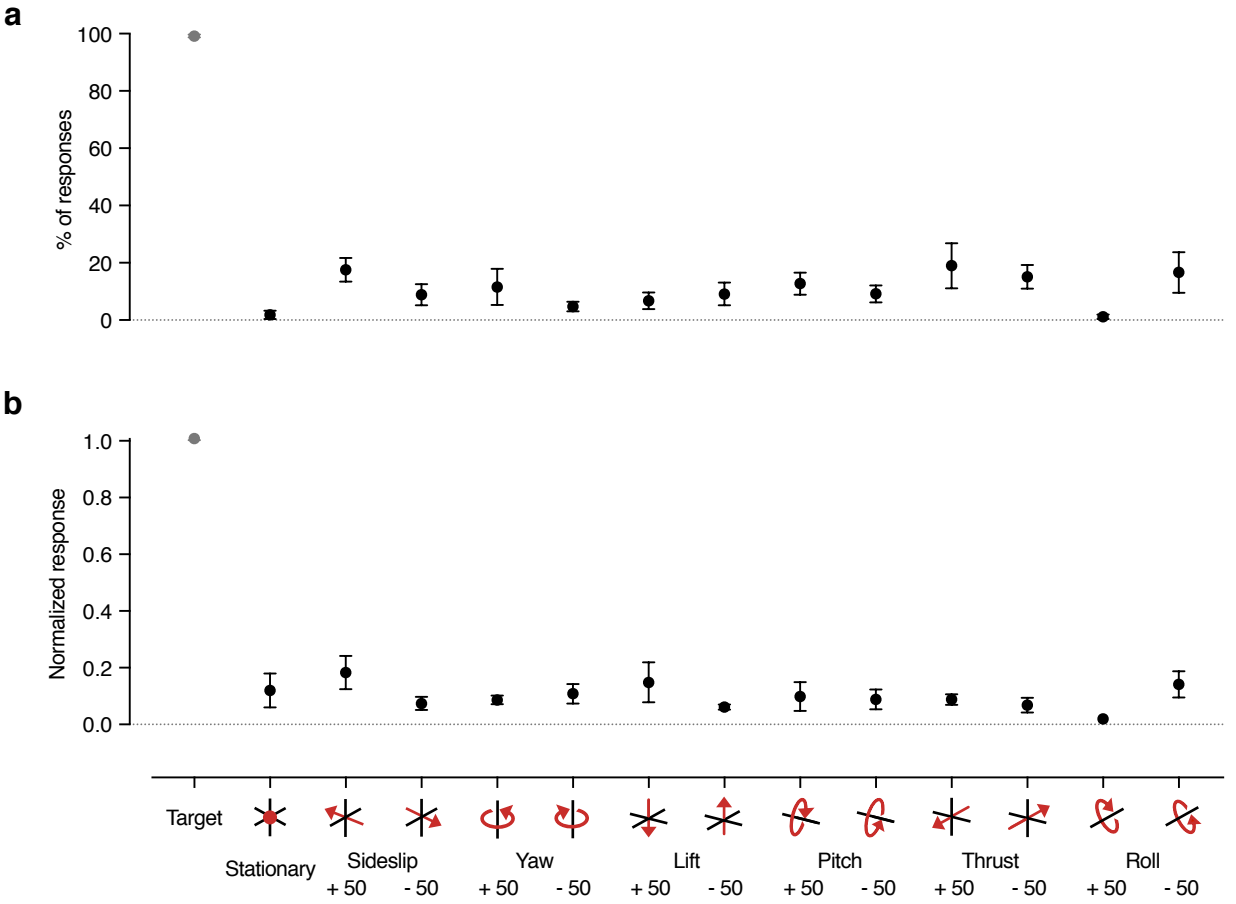
a
100
80
60
40
20
0
% of responses
b
1.0
0.8
0.6
0.4
0.2
0.0
Normalized response
Target
Stationary
Sideslip
+ 50
- 50
Yaw
+ 50
- 50
Lift
+ 50
- 50
Pitch
+ 50
- 50
Thrust
+ 50
- 50
Roll
+ 50
- 50